Title
The influence of future non-mitigated road transport emissions on regional ozone exceedences at global scale

Authors
Williams, JE
Hodnebrog, Ø
van Velthoven, PFJ
et al.

Publication Date
2014-06-01

DOI
10.1016/j.atmosenv.2014.02.041

Peer reviewed

Atmospheric Environment 89 (2014) 633–641

Contents lists available at ScienceDirect

Atmospheric Environment

journal homepage: www.elsevier.com/locate/atmosenv

The influence of future non-mitigated road transport emissions on regional ozone exceedences at global scale

J.E. Williams [a,*], Ø. Hodnebrog [b], P.F.J. van Velthoven [a], T.K. Berntsen [b,c], O. Dessens [d,e], M. Gauss [c,f], V. Grewe [g], I.S.A. Isaksen [c], D. Olivié [f,h], M.J. Prather [i], Q. Tang [i,j]

[a] Royal Netherlands Meteorological Institute, Wilhelminalaan 10, 3732 GK De Bilt, The Netherlands
[b] Center for International Climate and Environmental Research-Oslo (CICERO), Oslo, Norway
[c] Department of Geosciences, University of Oslo, Norway
[d] Centre for Atmospheric Science, Department of Chemistry, University of Cambridge, UK
[e] UCL Energy Institute, University College London, London, UK
[f] Norwegian Meteorological Institute, Oslo, Norway
[g] German Centre for Air and Space Travel, Institute of Atmospheric Physics, Oberpfaffenhofen, Germany
[h] Météo-France, GAME/CNRM, Toulouse, France
[i] Department of Earth System Science, University of California, Irvine, USA
[j] Department of Biological and Environmental Engineering, Cornell University, Ithaca, USA

HIGHLIGHTS

- Regional trend studies regarding NO_x emissions across all transport and industrial sectors between 2000 and 2050.
- Assessment of global air quality for the year 2000 using the EC recommendation for exceedence limit.
- Identification of the most sensitive world regions in terms of a policy failure for road traffic emissions.
- Assessment to whether mitigation of road traffic emissions is crucial for meeting future air quality standards.

ARTICLE INFO

Article history:
Received 5 August 2013
Received in revised form
16 February 2014
Accepted 19 February 2014
Available online 19 February 2014

Keywords:
Air quality
Road traffic emissions
3D global chemistry modelling
Future trends

ABSTRACT

Road Transport emissions (RTE) are a significant anthropogenic global NO_x source responsible for enhancing the chemical production of tropospheric ozone (O_3) in the lower troposphere. Here we analyse a multi-model ensemble which adopts the realistic SRES A1B emission scenario and a "policy-failure" scenario for RTE (A1B_HIGH) for the years 2000, 2025 and 2050. Analysing the regional trends in RTE NO_x estimates shows by 2025 that differences of 0.2–0.3 Tg N yr^{-1} occur for most of the world regions between the A1B and A1B_HIGH estimates, except for Asia where there is a larger difference of ~1.4 Tg N yr^{-1}. For 2050 these differences fall to ~0.1 Tg N yr^{-1}, with shipping emissions becoming as important as RTE. Analysing the seasonality in near-surface O_3 from the multi-model ensemble monthly mean values shows a large variability in the projected changes between different regions. For Western Europe and the Eastern US although the peak O_3 mixing ratios decrease by ~10% in 2050, there is an associated degradation during wintertime due to less direct titration from nitric oxide. For regions such as Eastern China, although total anthropogenic NO_x emissions are reduced from 2025 to 2050, there is no real improvement in peak O_3 levels. By normalizing the seasonal ensemble means of near-surface O_3 (0–500 m) with the recommended European Commission (EC) exposure limit to derive an exceedence ratio (ER), we show that ER values greater than 1.0 occur across a wide area in the Northern Hemisphere for boreal summer using the year 2000 emissions. When adopting the future A1B_HIGH estimates, the Middle East exhibits the worst regional air quality, closely followed by Asia. For these regions the area of exceedence (ER > 1.0) for 2025 is ~40% and ~25% of the total area of each region, respectively. Comparing simulations employing the various scenarios shows that unmitigated RTE increases the area of exceedence in the Middle East by ~6% and, for Asia, by ~2% of the total regional areas. For the USA the area of exceedence approximately doubles in 2025 as a result of un-mitigated RTE, with the most exceedences occurring in the southern USA. The effects across the various

* Corresponding author. Royal Netherlands Meteorological Institute, Wilhelminalaan 10, 3732 GK De Bilt, The Netherlands.
E-mail address: williams@knmi.nl (J.E. Williams).

http://dx.doi.org/10.1016/j.atmosenv.2014.02.041
1352-2310/

regions implies that unmitigated RTE would have a detrimental effect on regional health for 2025, and potentially offset the benefits introduced by mitigating e.g. international shipping emissions. By 2050 the further mitigation of non-transport emissions results in much cleaner air meaning that mitigation of RTE is not critical for achieving the defined limits in many world regions.

1. Introduction

High concentrations of tropospheric ozone (O_3) near the Earth's surface has a range of detrimental effects including increased mortality (Bell et al., 2004), decreased crop production (Hollaway et al., 2012) and impaired visibility (Sillman, 2003). Recently, it has been shown that nitrogen oxide emissions (NO_x) from road transport have been an important contributor towards tropospheric O_3 mixing ratios in the lower troposphere at the beginning of this century (Hoor et al., 2009). Estimates in the SRES A1B emission scenarios (Nakicenovic et al., 2000) predict a reduction in global Road Transport Emissions (RTE) of NO_x from ~9 Tg N yr^{-1} (2000) to ~7 Tg N yr^{-1} (2025), followed by a further reduction to ~2 Tg N yr^{-1} (2050), assuming the efficient application of mitigation technologies. It is estimated that A1B SRES has provided the most realistic emission estimates to date from the different SRES scenarios, where the integrated global anthropogenic emissions are thought to have exceeded the A1B estimates up to 2008 (Garnet et al., 2008). More recently there has been a decline in anthropogenic NO_x emissions associated with the global economic crisis, where trends observed from space have shown there has been a significant impact of economic activity on regional emission trends (e.g. Lin and McElroy, 2011). The assumed reduction in global RTE for future decades means that their influence on atmospheric composition could diminish (Koffi et al., 2010). However, there is the possibility that the estimated reductions in RTE are not attained, resulting in a so-called 'policy-failure' scenario (A1B_HIGH). Given the ubiquitous use of road transport in many world regions such a 'policy-failure' has the potential to prolong the time-scale needed in achieving air quality targets, which have been legislated for in future decades.

Here we analyse the results of a multi-model ensemble study performed using large scale atmospheric chemistry-transport models as part of the recent EU-QUANTIFY project (Quantifying the Climate Impact of Global and European Transport Systems; http://www.pa.op.dlr.de/quantify/) where the focus was on the effects of Transport Emissions (TE) on global atmospheric composition. First we analyse the regional trends in NO_x emissions between 2000 and 2050 as estimated in the A1B and the "policy-failure" scenario regarding RTE. Then we investigate the consequences A1B_HIGH would have on regional air quality in terms of tropospheric O_3 for a number of important world regions over the coming decades. By using exposure recommendations provided by the EC regarding safe air-quality standards for O_3, we subsequently determine which world regions exhibit the highest sensitivity towards unmitigated RTE and assess the extent to which this affects exceedences above the defined threshold that is deemed safe.

2. Trends in regional NO_x emission estimates between 2000 and 2050

By examining the global trends in NO_x emissions from each of the different transport sectors defined in the SRES A1B and A1B_HIGH scenarios (Nakicenovic et al., 2000; Hodnebrog et al., 2011) it has been shown that A1B_HIGH estimates that the road sector will release the highest global NO_x emissions across all transport sectors by 2025 (equal to ~9.5 Tg N yr^{-1}) and will be the second most important by 2050 after shipping (equal to ~3 Tg N yr^{-1}). Fig. 1 shows the global surface distribution of RTE annual NO_x emissions for the year 2000. The RTE NO_x from Europe, the US and Taiwan/Korea/Japan are an order of magnitude larger than those estimated for either India or China.

Here we decompose the global trends in RTE NO_x for a number of world regions containing large urban centres, namely: Europe (20°W–30°E, 37–70°N), the USA (60–140°W, 30–54°N), Asia (60–140°E, 10°S–60°N), South America (30–90°W, 40°S–10°N), Africa (20°W–50°E, 14°N–36°S) and the Middle East (16–60°E, 14–40°N). Each of these regions is clearly defined in Fig. 1 and shown as the solid lines. The smaller sub-regions shown within the black dashed lines are used for analysis in Section 4.

Fig. 2 shows the emission trends across the timeline 2000–2050 for both the A1B and A1B_HIGH. For clarity the trend in the absolute differences in RTE between the A1B and A1B_HIGH are shown. in the upper right panel in Tg N yr^{-1}. Also shown are the corresponding regional NO_x trends for shipping, aircraft (scaled up five-fold) and the cumulative emissions from industrial/domestic/biomass burning sectors (hereafter referred to as the non-transport sector (NTS)). Although the largest regional NO_x emissions come from the NTS, integrating the contribution across all transport sectors shows that the total contribution approaches ~50% of that from the NTS in 2025. As for the global emission trends shown in Hodnebrog et al. (2011), the contribution to regional NO_x from RTE in the A1B_HIGH scenario dominates the other transport sectors in 2025. This dominance of RTE is in spite of the rapid increase in air transport, which introduces a rather low regional NO_x emission. For 2050, the NTS is either equal to or lower than that in 2025 due to mitigation and the implementation of technological developments. For RTE NO_x emissions become either comparable to (e.g. South America) or lower than (e.g. Asia) those from the shipping sector.

Analysing the regional NO_x emission trends shown in Fig. 1 reveals that the Asian region has the largest RTE of NO_x across the entire timeline, with the annually integrated RTE being approximately double those of Europe and the USA for future decades. For A1B_HIGH, this results in an extra emission of ~1.4 Tg N yr^{-1} from Asia by 2025, which decreases to ~0.4 Tg N yr^{-1} by 2050. For the Middle East (ME), A1B_HIGH results in this region becoming the second most important region for RTE by 2050 and for South America, A1B_HIGH results in the trend in RTE exhibiting a modest increase by 2025 (equating to differences of ~0.2–0.3 Tg N yr^{-1}). For most of the world regions shown the additional NO_x from RTE A1B_HIGH falls to ~0.1 Tg N yr^{-1} by 2050 when compared to A1B, thus being negligible in terms of total global N emissions.

3. Methodology

3.1. Multi-model ensemble

The multi-model ensemble used here is similar to that used to assess the present-day and future impact of TE on tropospheric composition and oxidative capacity (Hoor et al., 2009; Hodnebrog et al., 2011, 2012). For the purpose of this study the ensemble includes five independent members, these being: TM4, OSLO CTM-2,

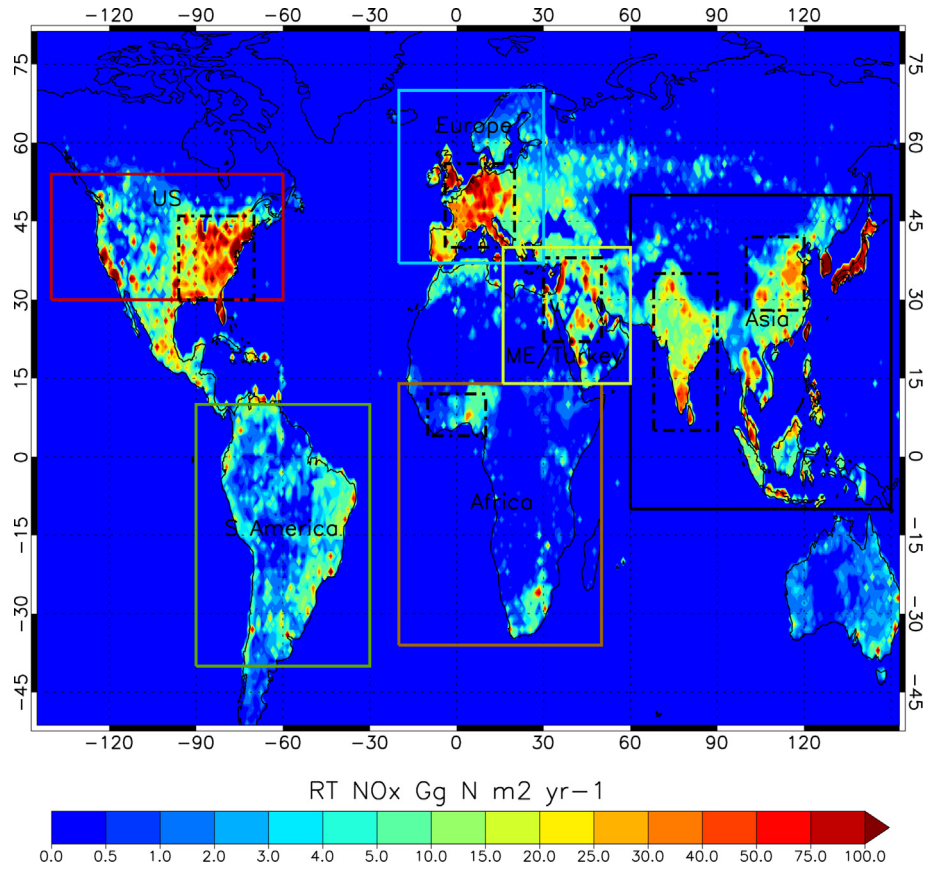

Fig. 1. The global distribution of annually integrated NO_x emissions from RTE for the year 2000. Also shown are the regions used for the regional trend analysis.

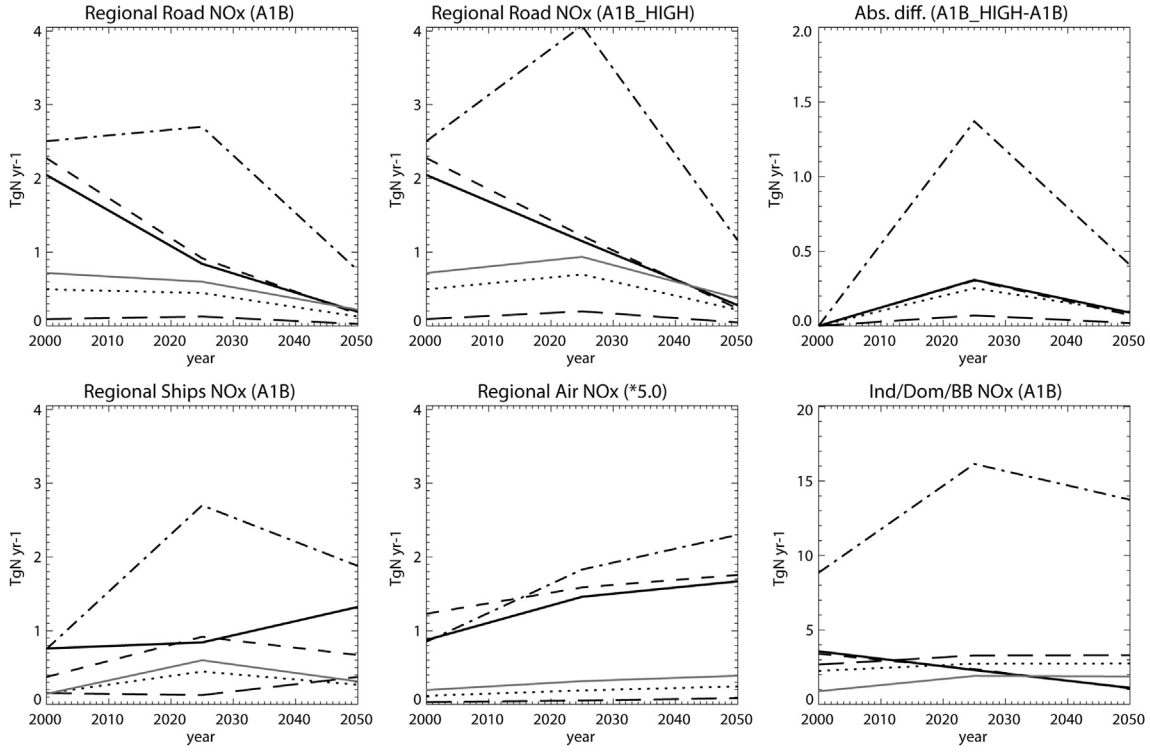

Fig. 2. Regional trends in annually integrated NO_x emissions (in Tg N yr^{-1}) from road traffic between 2000 and 2050 as defined in SRES A1B (top left panel) and A1B_HIGH (top middle panel) emission scenarios. The difference between scenarios is given in the top right panel. Also shown are the regional trends in NO_x emissions from shipping (bottom left panel), aircraft (bottom middle panel) and the NTS (bottom right panel). The aircraft NO_x emissions are scaled up by a factor of 5 for clarity. Key to world regions shown: Europe (dashed), the USA (solid), Asia (dash-dot), the Middle East (grey line), South America (dotted) and Africa (long dash).

p-TOMCAT, MOCAGE and UCI CTM. We perform simulations using the SRES A1B anthropogenic emission estimates derived for the years 2000, 2025 and 2050, where Table 1 provides an overview of all the simulations which are used and the source of the emission estimates. It should be noted that the nature of the models is such that sub-grid variability in chemical regimes is not accounted for e.g. the differences in the variability in composition between polluted plumes, urban centers and the surrounding suburbs is not captured. Moreover, no daily or weekly cycle has been implemented in the model ensemble for RTE due to the difficulty in defining the weekly variability due to differences in the cultural and religious practices between world regions. Another limitation is that these results are sensitive to the horizontal resolution adopted by each of the ensemble members for the calculation of the photo-chemical production of O_3 (Wild and Prather, 2006), meaning higher resolution simulations may alter the findings presented here.

In order to differentiate the effects due to the various TE from those introduced by meteorological variability and potential climate change we fix the meteorology for the year 2003 across the entire timeline. There is homogeneity between the different models in that all are driven by ECMWF operational meteorological data. The models used either include only tropospheric chemistry (TM4, p-TOMCAT, UCI) or both stratospheric and tropospheric chemistry (Oslo CTM-2, MOCAGE). For brevity, we refer the reader to the detailed model descriptions provided in Hodnebrog et al. (2011). One major benefit of using a model ensemble is that any model biases and deficiencies are minimized by averaging the values attained from all members of the ensemble. For instance, resident mixing ratios of O_3 in the boundary layer in a large-scale CTM are sensitive to the description of the dry deposition term (Ordóñez et al., 2010), with the model ensemble used here utilizing a range of different parameterizations to calculate the loss to the surface. The output from each model is then interpolated onto 40 levels at a T42 resolution for the analysis.

The performance of the various members included in the model ensemble has been validated by comparing the present day global distribution and seasonality of tropospheric O_3 against the climatology assembled from ozonesonde measurements for the 1990's (Logan, 1999), as shown in Hodnebrog et al. (2011). This provides some confidence that the ensemble captures both the seasonal and latitudinal variability in the distribution of tropospheric O_3 when using the present-day emission scenarios provided in the EU-QUANTIFY project.

Table 1
A definition of each of the model simulations performed for this study. For the biogenic emissions climatological values averaged between the years 2000–2003 are used (Hoor et al., 2009) and for biomass burning emissions estimates for the year 2000 are taken from the GFEDv1 inventory (Van der Werf et al., 2006) using multi-year averaged activity data from Andreae and Merlet (2001). The meteorological fields are fixed at the year 2003 throughout. Lightning NO_x emissions are constrained at $\sim$5 Tg N yr^{-1}. The chemical species for which RTE contribute are NO_x, CO, SO_2 and Non-methane Hydrocarbons.

Anthropogenic emission scenario	Reference	Simulation
2000	Olivier et al. (2005) Van Aardenne et al. (2005) Borken et al. (2007) Endresen et al. (2007)	PRESENT
2025	Nakicenovic et al. (2000) Uherek et al. (2010) Eide et al. (2007) Owen et al. (2010)	A1B 2025
2025 + High RTE	As for A1B 2025	A1B HIGH 2025
2050	Nakicenovic et al. (2000) Uherek et al. (2010) Eide et al. (2007) Owen et al. (2010)	A1B 2050
2050 + High RTE	As for A1B 2050	A1B HIGH 2050

3.2. Exceedence ratio for tropospheric O_3

To assess whether the distribution of near-surface (0–500 m) O_3 simulated by the model ensemble results in regional exceedences of air quality standards, we use a method where we normalize the monthly mean mixing ratios by the recommended 8-hourly limit provided by the EC of 60 ppb exposure for a period of 25 days in any one year (EC, 2008). In this paper we define the Exceedence Ratio (ER) as the near-surface O_3 mixing ratios normalized by this EC standard of 60 ppb. There is typically a strong diurnal cycle present for tropospheric O_3 related to the daily variation in photochemical activity meaning that the seasonal average could include more than 25 days where the EC recommendations are broken.

4. Results

4.1. Seasonality in O_3 and NO mixing ratios over populated regions

In Fig. 3 we show the annual variation in the monthly mean near-surface mixing ratios for O_3 and NO from the multi-model ensemble over six sub-regions as shown in Fig. 1 (dashed black lines), namely: Western Europe (4°W–20°E, 40–56°N), Eastern US (70–96°W, 30–46°N), East China (100–120°E, 28–42°N), West Africa (10°W–10°E, 4–12°N), India (68–90°E, 5–35°N) and ME/Turkey (30–50°E, 22–38°N). Comparisons are made between PRESENT, A1B 2025 and A1B 2050. In the majority of models included in the ensemble NO_x emissions are introduced as NO. A clear anti-correlation exists between the seasonality of O_3 and NO due to titration of O_3 under high NO_x conditions. The magnitude of the seasonal variability is determined by the photochemical activity of each of the sub-regions, and the seasonality of biogenic and biomass burning NO_x emissions. Peaks in near-surface O_3 occur during boreal summertime in Western Europe, Eastern US, East China and the ME/Turkey, where resident mixing ratios are $\sim$100% higher than those during boreal wintertime. For West Africa, a minimum occurs during the boreal summertime in stark contrast to the other regions, due to seasonal biomass burning.

The mitigation of anthropogenic NO_x emissions in Western Europe and the Eastern US results in two seasonal features: (i) an increase in near-surface O_3 during boreal wintertime of $\sim$10 ppb (+30%) and (ii) a decrease in peak near-surface O_3 during boreal summertime of $\sim$5 ppb (−10%). Thus, these simulations show that, although there are improvements in the peak O_3 levels during boreal summertime similar to other multi-model studies (e.g. Collette et al., 2012), an additional consequence of mitigating NO_x emissions is a degradation in air quality in terms of near-surface O_3 during boreal wintertime. In part this is due to the convective venting of the boundary layer being much weaker at the northern mid-latitudes during the winter, thus accumulating the additional O_3 near the surface.

For East China, which exhibits the highest NO_x emissions in 2025 (c.f. Fig. 2), near-surface O_3 levels increase by a few ppb during boreal wintertime and by $\sim$10 ppb during boreal summertime. These increases in O_3 persist throughout the timeline, in spite of the projected decreases in cumulative anthropogenic NO_x emissions between 2025 and 2050. For the ME/Turkey, whose projected anthropogenic NO_x emissions follow a similar pattern to that shown for East China, peak near-surface O_3 values are highest for 2025. For the tropical sub-regions increases in peak near-surface O_3 levels occur by 2025, which dampens the seasonal cycle significantly for West Africa by contributing up to $\sim$20 ppb during August. For India

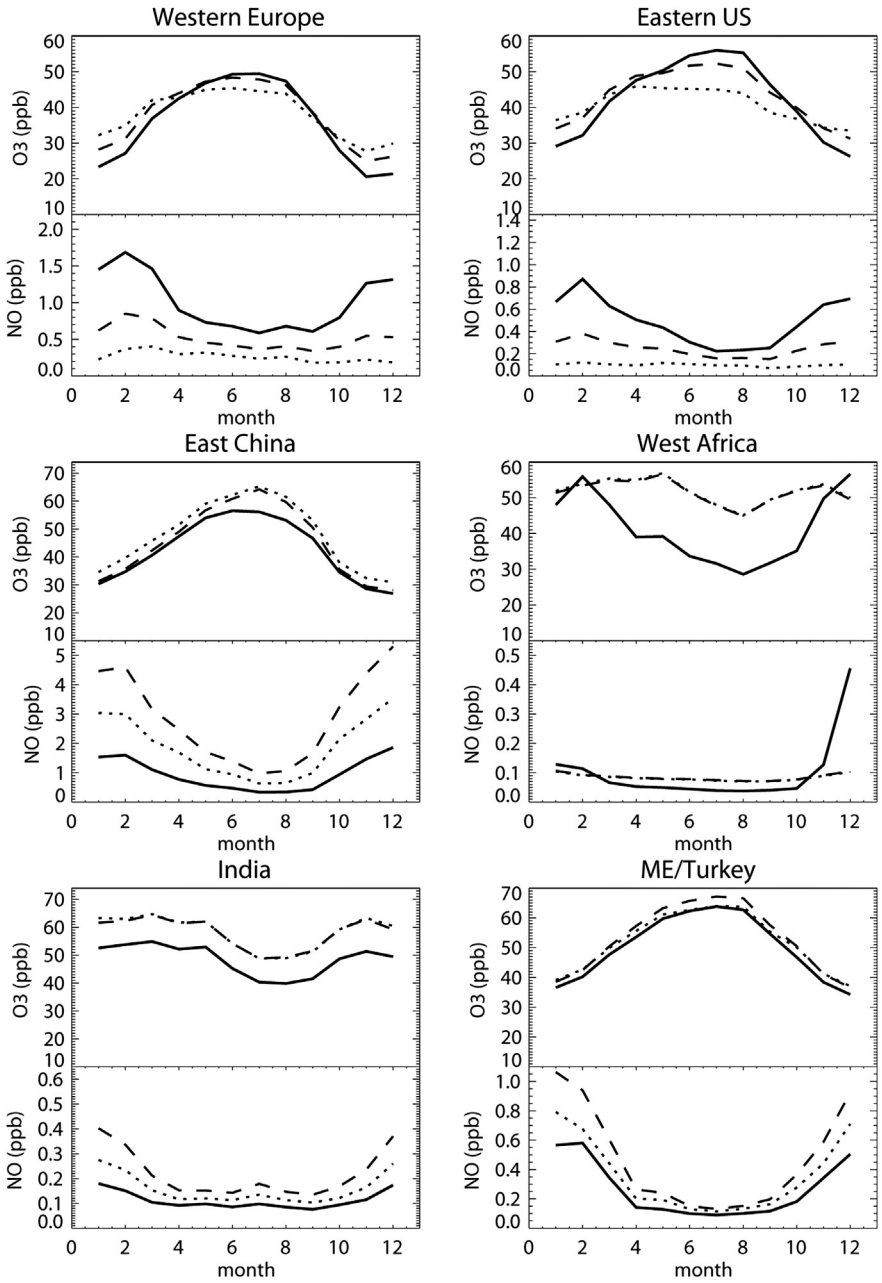

Fig. 3. The seasonal cycles in near-surface O_3 and NO for selected sub-regions shown in Fig. 1. Ensemble monthly means are provided for PRESENT (solid line), A1B 2025 (dashed line) and A1B 2050 (dotted line) annual cycles. The geographical limits of each region are given in the text.

increases in 2025 and 2050 appear as an offset of ~10 ppb throughout the year, where there is only a muted seasonal cycle.

4.2. Global distribution of exceedences for 2000

Fig. 4 shows the global seasonal distribution of ER for 2000 during both December–January–February (DJF) and June–July–August (JJA). The global distribution of near-surface O_3 in the multi-model ensemble is determined by the cumulative effect of emissions from all sources including natural (biogenic) activity and biomass burning, both of which exhibit strong seasonal cycles. The blue (in web version)/green (in web version) regions represent tropospheric air with ER $<$ 1.0, whereas the yellow (in web version)/red (in web version) regions represent areas with ER $>$ 1.0. As shown in Fig. 3 above, there is a clear seasonal impact evident in the integrated area where exceedences occur. This results in exceedences over wide areas of Europe, the USA, Asia and the ME during season JJA. For Africa, the worst exceedences shift in line with the change in the regional biomass burning activity. Mitigation of emissions from this source is much less realistic than that from either the industrial or transport sectors due to the importance for food production. We therefore limit the following discussion to the impact of A1B_HIGH on the air quality during JJA in global regions experiencing high regional anthropogenic emissions, which represents the maximal effect throughout the year.

When examining the seasonal distribution of the ER for 2025 and 2050 simulated using the A1B emission estimates (not shown), the strong mitigation practices associated with NTS emissions for both Europe and the USA means that ER values typically reach between 0.7 and 1.1 (i.e.) somewhat lower than the maximal values

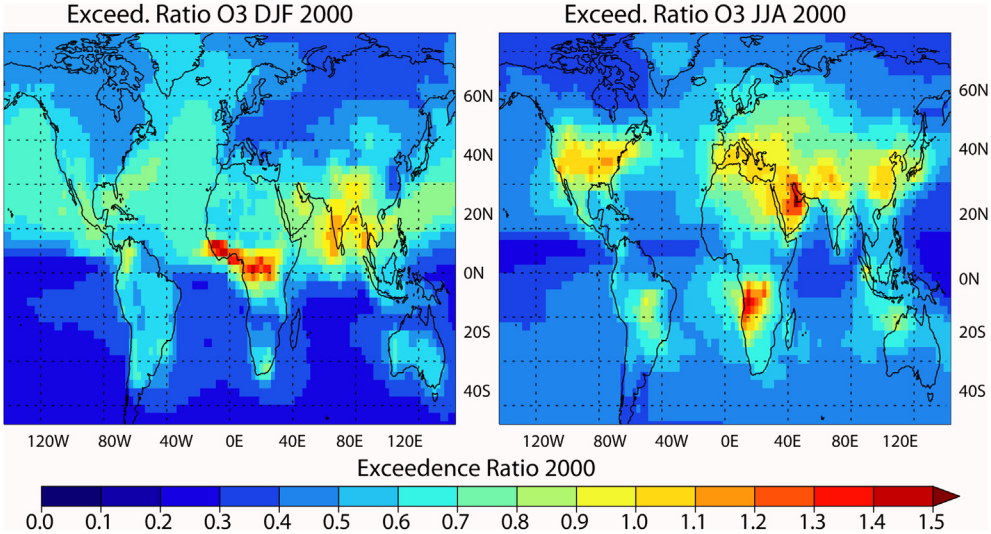

Fig. 4. The global distribution of the Exceedence Ratio (ER) for near-surface O_3 for DJF (left) and JJA (right) when using the 2000 emission estimates as calculated using the ensemble mean.

shown for 2000. Examining other developing regions such as South America, the growth in the total RTE is rather small (c.f. Fig. 2) considering the large area over which they are distributed, meaning that there are rarely exceedences at continental scale. Other regions such as Asia show a substantial increase in the area of exceedence related to increasing anthropogenic NTS emissions. For our analysis we investigate the future exceedences which occur in both developed and developing regions. Therefore, we choose two regions which have an improvement in air-quality and two regions which experience significant exceedences in future decades. The four global regions which are selected are: (i) Europe, which has low air quality over the Mediterranean for the present day, (ii) the USA, which has the highest RTE for 2000, (iii) Asia, which has the largest area of exceedences when adopting future emission scenarios and (iv) the Middle East, which exhibits notoriously high near-surface O_3 values during JJA (Lelieveld et al., 2009). It should be noted that these regions are somewhat larger than the smaller sub-regions used to analyse the seasonality in the multi-model ensemble monthly mean near-surface O_3 behaviour in Section 4.1 and exhibit a more varied change across the timeline. For these global regions we determine the impact that applying A1B_HIGH has on regional air quality during JJA and show the variations in exceedences for the years 2025 and 2050.

4.3. Present and future exceedences in Europe and the USA

Fig. 5 shows the ER for 2000 over both Europe and the USA, including the surrounding oceans, as calculated by the multi-model ensemble, along with the associated differences for 2025 and 2050.

For Europe highest ER values occur over the Mediterranean basin, which experiences high photochemical activity, high shipping emissions and the transport of polluted air from Central and Southern Europe. For 2025, there are limited increases in the ER values for A1B_HIGH of 0.05–0.1 occurring over North Africa and around Paris and London, which exhibit high population density and high resident NO_x emissions. Comparing absolute differences between A1B and A1B_HIGH (not shown) reveals that unmitigated RTE reduces the resident mixing ratios of near-surface O_3 around Paris by ~1% as a result of enhanced chemical titration of O_3 by the additional NO released (Kurtenbach et al., 2012). The largest decreases in ER during 2025 of <0.1 occur over the Mediterranean and appear in spite of the projected increase in shipping emissions (Eide et al., 2007; Hodnebrog et al., 2011), with unmitigated RTE contributing an additional ~1–2 ppb (not directly shown). This is due to cleaner air being transported from the continent out over the region as a result of the effective mitigation of the NTS emissions in e.g. the Po Valley in Italy (c.f. Fig. 2).

For 2050 (right panels) the increases in ER around the UK and Paris persist, where the additional titration effect disappears causing a small increase of <0.5 ppb in near-surface O_3 across Scandinavia and above the seas surrounding North–West Europe (not shown). For the rest of Europe the ER values fall significantly by 0.1–0.3 indicating significant reductions in the seasonal mixing ratios of between 6 and 18 ppb. Therefore, by 2050 the influence of unmitigated RTE is not crucial for meeting air quality standards in Europe because of the measures taken with respect to the NTS (c.f. Fig. 1). In Table 2 we provide the fraction of grid cells within Europe which exceed the EC recommendations. Here there is an increase in exceedences from 9.2% to 11.2% due to unmitigated RTE in 2025, with the difference in the impact falling to less than a percent for 2050.

For the USA there is an area of exceedence from the East to the West Coast, with some southern states exhibiting ER values of between 1.1 and 1.2 (i.e.) near-surface O_3 mixing ratios reach 72 ppb. Again, the strong photochemical activity which occurs at the more southern latitudes under high NO_x conditions enhances the in-situ production of tropospheric O_3. For 2025, mitigation of NTS emissions reduces the ER values by up to 0.1, although looking at the distribution of the ER values for 2000 reveals that exceedences still occur in the southern US, in spite of the decrease in NTS emissions. Table 2 shows that unmitigated RTE would result in an approximate doubling of the area for which exceedences occur from 4.0% to 7.6% of the total area selected, adding an additional 1–2 ppb to the surface mean mixing ratios across a wide area south of 45°N. This means that mitigating RTE seems crucial for meeting EC air quality standards when applied to the US. For 2050 (right panels), a further reduction in anthropogenic NO_x across all sources results in substantial decreases in ER across the whole of the USA, thus no exceedences occur even in the scenario with unmitigated RTE.

4.4. Present and future exceedences around the Middle East and Asia

Fig. 6 shows the distribution of ER for 2000 across the ME/Turkey, including parts of the Mediterranean basin and also the

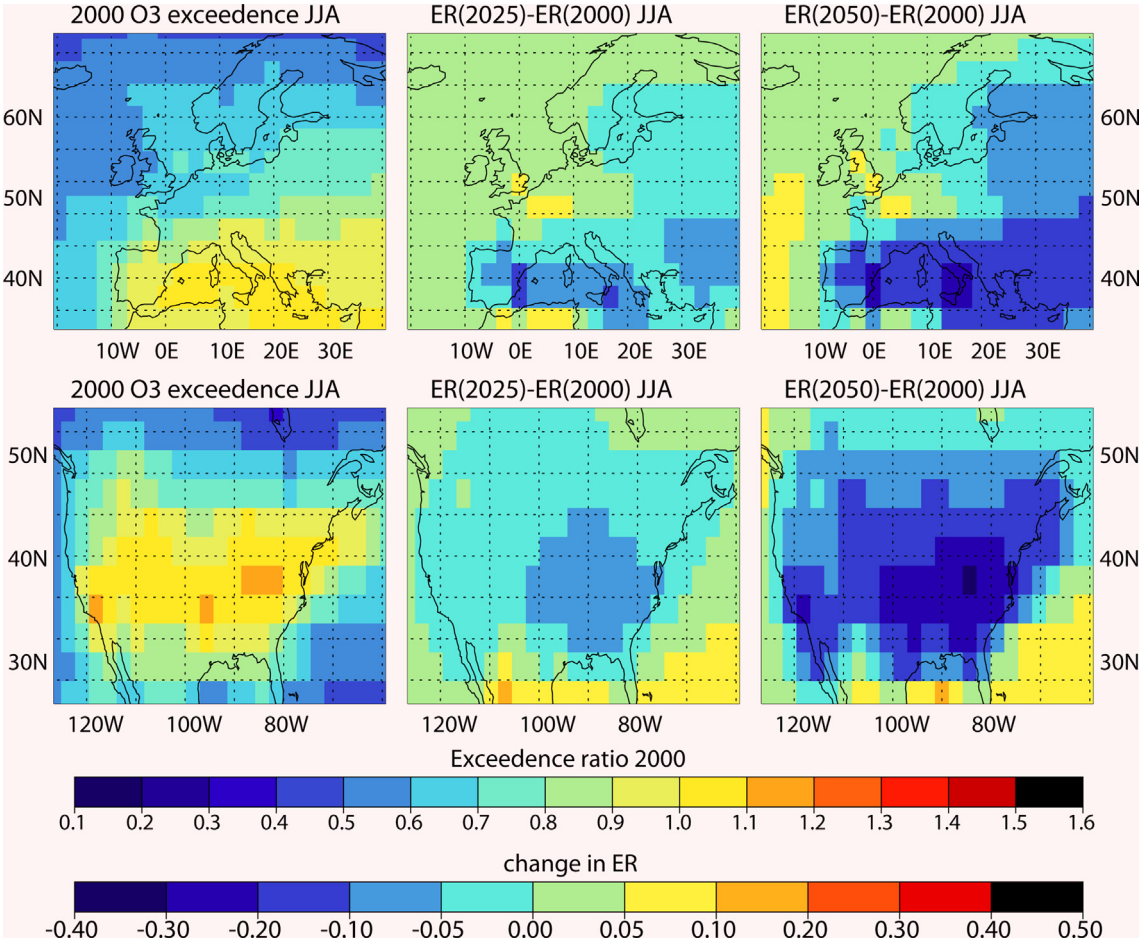

Fig. 5. The ER values for Europe (top left) and the USA (bottom left) as calculated in the multi-model ensemble for PRESENT. The changes in the ER for 2025 (middle) and 2050 (right) for the A1B_HIGH scenario are also shown for each region.

Asian region. The differences in the ER between 2000 and A1B_HIGH for 2025 and 2050 are also shown to assess the changes in ER predicted for future decades.

For 2000, there are exceedences in the ME over a wide area including Egypt, Iraq, Jordan and Israel, with the maximum ER ($>$1.5) occurring around Qatar, Bahrain and the Gulf of Oman. These maximal ER values equate to near-surface O_3 mixing ratios of up to 90 ppb for a substantial part of the season. When integrating exceedences for the entire region, Table 2 shows that ~40% of the total area in the region exhibits ER values higher than 1.0. For 2025, the near-surface mixing ratios increase to almost ~100% above the EC recommendations, being in the range of 100–120 ppb over a wide area. There is also a southerly shift of the exceedences away from the Mediterranean towards the Gulf of Oman, extending down towards Africa, which has the potential to alter crop yields and shifting more over the land leading to an increase in the exposure of the local population to low quality air. This southerly shift is in part due to the mitigation of NTS emissions outside the region, which reduces the transport of O_3 rich air into the Mediterranean basin. The effect of unmitigated RTE is to increase the area of exceedences by ~6% (Table 2), therefore exerting a significant effect on regional air quality.

For 2050, the further mitigation of European emissions improves air quality over Turkey, Lebanon and Israel significantly as the timeline progresses. In part, this is also due to the reduction in shipping emissions for the region as shown in Fig. 2. The maximal ER values decrease somewhat, where there is also an improvement in local air quality for countries in North Africa which border the Mediterranean. For the ME/Turkey, unmitigated RTE increases the total area of exceedence by ~2% (c.f. Table 2) compared to A1B, although an increase in ER values occurs over urban areas, again exposing the population to higher O_3 levels compounding the potential health effects. Here unmitigated RTE increase the resident mixing ratios of O_3 by between 1 and 3 ppb. The differences in the ER values between 2025 and 2050 are predominantly due to the changes which occur across the different transport sectors (c.f. Table 2), where the NTS component remains almost constant. Compared to 2025 the maximal ER values decrease by ~0.1 and the area of exceedence falls to ~31% of the total regional area shown. Therefore, although the increase in the number of grid cells for which exceedences occur is rather small in relative terms, analysing the trends in NO_x emissions between the different transport sectors shows that unmitigated RTE does have the potential to offset any improvements in air quality that would occur over the land due to a reduction in shipping emissions. Even for 2050 a wide area near the Persian Gulf remains polluted. Considering the rather small NTS contribution for the region (c.f. Fig. 2) any improvement in air quality must be gained by changing local TE, with RTE being an obvious candidate.

For the Asian region the most polluted regions when adopting the 2000 emissions are around the Ganges valley in Northern India and towards East China. The other regions are relatively clean, especially over the oceans, with the integrated exceedences only covering ~8% of the region shown. Moreover, the maximum ER

Table 2
The fractional area of exceedence above the EC air quality standards for tropospheric O_3 during JJA. For a definition of the simulations the reader is referred to Table 1.

Simulation	Europe	USA	Middle East	Asia
PRESENT	0.116	0.160	0.396	0.086
A1B 2025	0.092	0.040	0.342	0.232
A1B_HIGH 2025	0.112	0.076	0.401	0.248
A1B 2050	0.083	0.000	0.310	0.225
A1B_HIGH 2050	0.088	0.000	0.326	0.238

values in the region of 1.3–1.4 are somewhat lower than that for the ME/Turkey, possibly due to stronger convective uplift of pollutants out of the boundary layer due to Monsoon activity. For the future A1B_HIGH simulations, there is a substantial increase in the area of exceedences to ~25% of the region for 2025, remaining essentially unchanged for 2050. This is due to the large increases in emissions from the NTS related to e.g. energy production, construction and industrial manufacturing, with the trend in NTS emissions showing a doubling by 2025 followed by a reduction to ~150% of the A1B estimates for 2000 by 2050. This reduction in NTS is then subsequently offset by the growth in regional shipping emissions resulting in no net decreases in the number of exceedences over the timeline. Again, taking differences in the ER ratios between the A1B and A1B_HIGH simulations reveals that there is an increase in the exceedence area of ~2%, which equates to a larger area than that for the ME/Turkey due to the size of each respective region.

5. Conclusions

In this study we have used a multi-model ensemble of large-scale atmospheric chemistry models, which adopts the realistic SRES A1B emission scenario and a "policy-failure" scenario (A1B HIGH) for road traffic emissions (RTE), to differentiate the effects of unmitigated road traffic emissions on regional air quality for various global regions. Analysing the regional trends in RTE NO_x estimates provided in the pessimistic SRES emission scenarios, shows that differences of 0.2–0.3 Tg N yr^{-1} occur in road transport emissions for most of the worlds regions in 2025, except for Asia (~1.4 Tg N yr^{-1}). For 2050, these differences fall to ~0.1 Tg N yr^{-1}, with shipping emissions becoming as important for many of the chosen regions. Analysing the seasonality in the multi-model ensemble mixing ratios for near-surface O_3 shows that for Western Europe and the Eastern US, the peak level monthly mean values which occur during boreal summertime are reduced by ~10% by 2050. For boreal wintertime, enhancements in near-surface O_3 of ~30% occur as a result of less titration by nitric oxide. For other regions, such as China and India, a degradation in air quality occurs throughout the year across the timeline, where the projected mitigation of anthropogenic NO_x emissions by 2050 does not necessarily result in a decrease in O_3 mixing ratios.

By normalizing the seasonal multi-model ensemble means of near-surface (0–500 m) O_3 with the recommended EC exposure limit to derive an exceedence ratio (ER), we show that ER values greater than 1.0 occur across a wide area in the Northern Hemisphere for boreal summer when adopting the 2000 emission

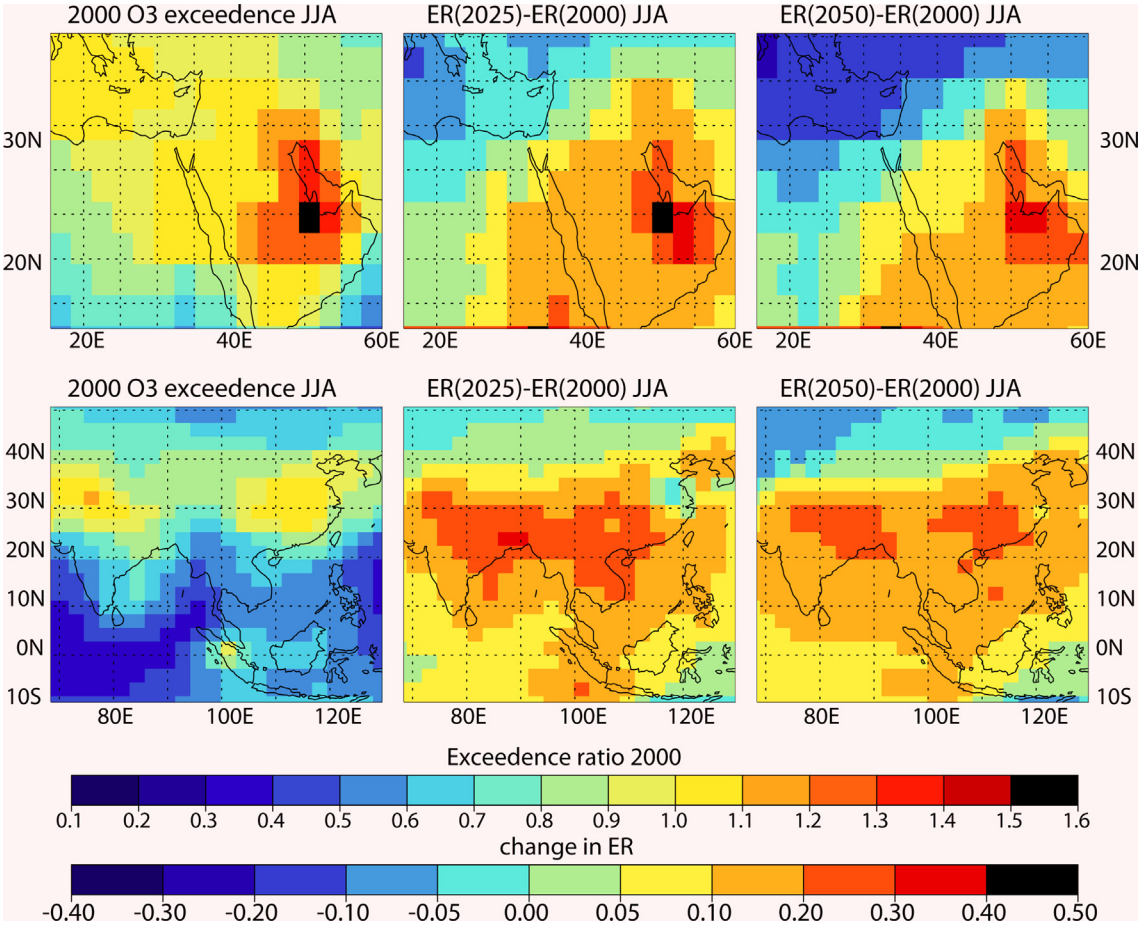

Fig. 6. The ER values for 2000 for the Middle East/Turkey (top left) and Asian (bottom left) regions as calculated in the multi-model ensemble. The changes in the ER for 2025 (middle) and 2050 (right) for the A1B scenario are also shown for each region.

estimates. When adopting the future A1B_HIGH estimates, a clear signature on air quality can be detected. The Middle East is the region which exhibits the worst air quality, closely followed by Asia. For these regions the area of exceedence (ER > 1.0) for 2025 is ~40% and ~25% of the total area of each region, respectively. Comparing simulations employing the various scenarios shows that unmitigated RTE increases the area of exceedences in the Middle East by ~6% and, for Asia, by ~2% of the total regional areas. For the USA, the number of exceedences approximately doubles in 2025 as a result of unmitigated RTE, with the most exceedences occurring in the southern US. The effect across the various regions implies that unmitigated RTE would have detrimental effect on regional health in these world regions for 2025, and potentially offsetting the benefits introduced by mitigating shipping emissions. By 2050, the further mitigation of non-transport emissions results in much cleaner air meaning the unmitigated RTE are not critical for achieving the defined limits in many world regions.

Acknowledgements

The authors acknowledge financial support from the QUANTIFY project which was funded by the European Union within the 6th Framework Programme under contract 003893 and the Norwegian Research Council.

References

Andreae, M.O., Merlet, P., 2001. Emissions of trace gases and aerosols from biomass burning. Global Biogeochemical Cycles 15, 955–966.

Bell, M.L., McDermott, A., Zeger, S.L., Samet, M., Dominici, F., 2004. Ozone and short-term mortality in 95 urban communities, 1987–2000. Journal of the American Medical Association 292, 2372–2378.

Borken, J., Steller, H., Mereti, T., Vanhove, F., 2007. Global and country inventory of road passenger and fright transportation – fuel consumption and emissions of air pollutants in year 2000. Transportation Research Record 2011, 127–136.

Collette, A., Granier, C., Hodnebrog, Ø., Jakobs, H., Maurizi, A., Nyiri, A., Rao, S., Amann, M., Bessagnet, B., D'Ahgiola, Gauss, M., Heynes, C., Klimont, Z., Meleux, F., Memmesheimer, M., Mieville, A., Rouil, L., Russo, F., Schucht, S., Simpson, D., Stordal, F., Tampieri, F., Vrac, M., 2012. Future air quality in Europe: a multi-model assessment of projected exposure to ozone. Atmospheric Chemistry and Physics 12, 10613–10630.

Europeamn Commission, Directive 2008/50/EC of the European Parliament and of the Council of 21 May 2008 on ambient air quality and cleaner air for Europe.

Eide, M.S., Endresen, O., Mjelde, A., Mangset, L.E., Gravir, G., 2007. Ship Emissions of the Future. Technical Report no 2007–1325. Det Norske Veritas, Høvik, Norway.

Endresen, O., Sorgard, E., Behrens, H.L., Brett, P.O., Isaksen, I.S.A., 2007. A historical reconstruction of ships fuel consumption and emissions. Journal of Geophysical Research: Atmospheres 112, D12301.

Garnet, R., Howes, S., Jotzo, S.F., Sheehan, P., 2008. Emissions in the platinum age: the implications of rapid development for climate-change mitigation. Oxford Review of Economic Policy 24 (2), 377–401.

Hodnebrog, Ø., Berntsen, T.K., Dessens, O., Gauss, M., Grewe, V., Isaksen, I.S.A., Koffi, B., Myrhe, G., Olivié, D., Prather, M.J., Pyle, J.A., Stordal, F., Szopa, S., Tang, Q., van Velthoven, P., Williams, J.E., Ødemark, K., 2011. Future impact of non-land based traffic emissions on atmospheric ozone and OH – an optimistic scenario and a possible mitigation strategy. Atmospheric Chemistry and Physics 11, 11293–11317. http://dx.doi.org/10.5194/acp-11-11293-2011.

Hodnebrog, Ø., Berntsen, T.K., Dessens, O., Gauss, M., Grewe, V., Isaksen, I.S.A., Koffi, B., Myrhe, G., Olivié, D., Prather, M.J., Stordal, F., Szopa, S., Tang, Q., van Velthoven, P., Williams, J.E., 2012. Future impact of traffic emissions on atmospheric ozone and OH based on two scenarios. Atmospheric Chemistry and Physics 12, 12211–12225.

Hoor, P., Borken-Kleefeld, J., Caro, D., Dessens, O., Endresen, O., Gauss, M., Grewe, V., Hauglustaine, D., Isaksen, I.S.A., Jöckel, P., Lelieveld, J., Myrhe, G., Meijer, E., Olivié, D., Prather, M.J., Schnadt-Poberaj, C., Shine, K.P., Staehelin, J., Tang, Q., van Aardenne, J., van Velthoven, P., Sausen, R., 2009. The impact of traffic emissions on atmospheric ozone and OH: results from QUANTIFY. Atmospheric Chemistry and Physics 9, 3113–3136.

Hollaway, M.J., Arnold, S.R., Challinor, A.J., Emberson, D., 2012. Intercontinental trans-boundary contributions to ozone-induced crop yield losses in the Northern hemisphere. Biogeosciences 9, 271–292.

Kurtenbach, R., Kleffman, J., Niedojadlo, A., Wiesen, P., 2012. Primary NO2 emissions and their impact on air quality in traffic environments in Germany. Environmental Sciences Europe 24 (12), 1–8.

Koffi, B., Szopa, S., Cozic, A., Hauglustaine, D., van Velthoven, P., 2010. Present and future impact of aircraft, road and shipping emissions on global tropospheric ozone. Atmospheric Chemistry and Physics 10, 11681–11705.

Lelieveld, J., Hoor, P., Jöckel, P., Pozzer, A., Hadjinicolaou, P., Cammas, J.-P., Beirle, S., 2009. Severe ozone air pollution in the Persian Gulf region. Atmospheric Chemistry and Physics 9, 1393–1406.

Lin, J.-T., McElroy, M.B., 2011. Detection from space of a reduction in anthropogenic emissions of nitrogen oxides during the Chinese economic downturn. Atmospheric Chemistry and Physics 11, 8171–8188.

Logan, J., 1999. An analysis of ozonesondes data for the troposphere: recommendations for testing 3-D models and development of a gridded climatology for tropospheric ozone. Journal of Geophysical Research 104, 16115–16149. http://dx.doi.org/10.1029/1998jd100096.

Nakicenovic, N., Davidson, O., Davis, G., Grübler, A., Kram, T., La Rovere, E.L., Metz, B., Morita, T., Pepper, W., Pitcher, H., Sankovski, A., Shukla, P., Swart, R., Watson, R., Dadi, Z., 2000. Special Report on Emissions Scenarios. Cambridge University Press, Cambridge, p. 599.

Olivier, J.G.J., van Aardenne, J.A., Dentener, F., Ganzeveld, L., Peters, J.A.H.W., 2005. Recent Trends in Global Greenhouse Gas Emissions: Regional Trends and Spatial Distribution of Key Sources in: Non-CO_2 Greenhouse Gases (NCGG-4). Millpress, Rotterdam, pp. 325–330.

Ordóñez, C., Elguindi, N., Stein, O., Huijnen, V., Flemming, J., Inness, A., Flentje, H., Katragkou, E., Moinat, P., Peuch, V.-H., Segers, A., Thouret, V., Athier, G., van Weele, M., Zerefos, C.S., Cammas, J.-P., Schultz, M.G., 2010. Global model simulations of air pollution during the 2003 European heat wave. Atmospheric Chemistry and Physics 10, 789–815.

Owen, B., Lee, D.S., Lim, L., 2010. Flying into the future: aviation emissions scenarios till 2050. Environmental Science and Technology 44, 2255–2260.

Sillman, S., 2003. Tropospheric ozone and photochemical smog. In: Holland, H.D., Turekian, K.K. (Eds.), Environmental Geochemistry, Treatise on Geochemistry, vol. 9. Elsevier-Pergammon, Oxford, pp. 407–432.

Uherek, E., Halenka, T., Borken-Kleefeld, J., Balkanski, Y., Berntsen, T., Borrego, C., Gauss, M., Hoor, P., Juda-Rezler, K., Lelieveld, J., Melas, D., Rypdal, K., Schmid, S., 2010. Transport impacts on atmosphere and climate: land transport. Atmospheric Environment 44, 4772–4816.

Van Aardenne, J.A., Dentener, F.J., Olivier, J.G.J., Peters, J.A.H.W., Ganzeveld, L.N., 2005. The EDGAR 3.2 Fast Track 2000 Dataset (32FT2000). Joint Research Center, Institute for Environment and Sustainability (JRC-IES), Climate Change Unit, Ispra, Italy available at: http://themasites.pbl.nl/images/Description_of_EDGAR_32FT2000(v8)_tcm61_46462.pdf.

Van der Werf, G.R., Randerson, J.T., Giglio, L., Collatz, C.J., Kasibhatla, P.S., Arellano Jr., A.R., 2006. Interannual variability in global biomass burning emission from 1997 to 2004. Atmospheric Chemistry and Physics 6, 3423–3441.

Wild, O., Prather, M.J., 2006. Global tropospheric ozone modelling: quantifying errors due to grid resolution. Journal of Geophysical Research 111, D11305.